

Search for new light vector boson using J/Ψ at BESIII and Belle II

Kayoung Ban,^{1,*} Yongsoo Jho,^{1,†} Youngjoon Kwon,^{1,‡} Seong
Chan Park,^{1,§} Seokhee Park,^{1,¶} and Po-Yan Tseng^{1,**}

¹*Department of Physics and IPAP, Yonsei University,
Seoul 03722, Republic of Korea*

Abstract

We investigate various search strategies for light vector boson X in $\mathcal{O}(10)$ MeV mass range using J/Ψ associated channels at BESIII and Belle II: (i) $J/\Psi \rightarrow \eta_c X$ with $10^{10} J/\Psi$ s at BESIII, (ii) $J/\Psi(\eta_c + X) + \ell\bar{\ell}$ production at Belle II, and (iii) $J/\Psi + X$ with the displaced vertex in $X \rightarrow e^+e^-$ decay are analyzed and the future sensitivities at Belle II with 50 ab^{-1} luminosity are comprehensively studied. By requiring the displaced vertex to be within the beam pipe, the third method results in nearly background-free analysis, and the vector boson-electron coupling and the vector boson mass can be probed in the unprecedented range, $10^{-4} \leq |\varepsilon_e| \leq 10^{-3}$ and $9 \text{ MeV} \leq m_X \leq 100 \text{ MeV}$ with 50 ab^{-1} at Belle II. This covers the favored signal region of ${}^8\text{Be}^*$ anomaly recently reported by Atomki experiment with $m_X \simeq 17 \text{ MeV}$.

arXiv:2012.04190v2 [hep-ph] 3 Mar 2021

* ban94gy@yonsei.ac.kr

† jys34@yonsei.ac.kr

‡ yjkwon63@yonsei.ac.kr

§ sc.park@yonsei.ac.kr

¶ seokhee.park@yonsei.ac.kr

** tpoyan1209@gmail.com

I. INTRODUCTION

The Standard Model (SM) is a successful theory describing physics at least up to the electroweak scale, having survived more than 40 years of various experimental tests. However, there still remain a handful number of experimental and observational claims that indicate discrepancies from the SM predictions and consequently request extension of the SM: non-zero mass of neutrinos [1], anomalous magnetic moment of muon, $(g - 2)_\mu$ [2, 3], existence of dark matter (DM) [4], ¹ and baryon vs. antibaryon asymmetry of the universe [6, 7]. There have been discussions of extending the SM by gauging the lepton number, e.g. $L_\mu - L_\tau$ or $L_e - L_\tau$ [8], intending to explain DM [9, 10], the muon anomalous magnetic moment $(g - 2)_\mu$ [11–14], and more recently EDGES 21cm anomaly [15]. The extension gives rise to a leptophilic light vector boson, dubbed as X in this paper. We note that the X boson may couple to the quarks via interactions with unknown heavy fermions that mix with SM quarks [16]. It may then be responsible for the recent anomaly from the KOTO experiment in $K_L \rightarrow \pi^0 \nu \bar{\nu}$ [17–20] and also the anomaly from the Atomki experiment in both ${}^8\text{Be}^*$ and ${}^4\text{He}^*$. The preferred mass of X for these cases is in sub-GeV range; in particular $m_X \simeq 17$ MeV for Atomki [21, 22].

High luminosity lepton colliders provide ideal environments to test for such light X boson. Thanks to less severe QCD backgrounds, the lepton colliders have definite advantages over hadron colliders even when the X boson has feeble couplings with the SM particles. In this paper, we take the lepton colliders, BESIII and Belle II, and study the search strategies of X . In particular, we focus on the channels in association with a J/Ψ meson, which will be enormously produced at BESIII and also at Belle II, thereby leaving the signals of X in various channels:

- At BESIII, up to now, 10^{10} J/Ψ events are collected, thus provide an excellent probe to study the J/Ψ rare decays to the X boson.
- At Belle II, even though less number of J/Ψ are expected, we use the process $e^+e^- \rightarrow \ell^+\ell^- J/\Psi \rightarrow \ell^+\ell^- \eta_c X \rightarrow \ell^+\ell^- \eta_c e^+e^-$ ($\ell = e$ or μ), in which J/Ψ and η_c are inferred by the recoil masses of $\ell^+\ell^-$ and $\ell^+\ell^- e^+e^-$, respectively.
- At Belle II, we also use the channel $e^+e^- \rightarrow X + J/\Psi$ where the X bosons will leave signals with displaced vertices. Due to higher center-of-mass (CM) energy at Belle II, the X boson will be boosted and travel several millimeters before it decays into e^+e^- .

The rest of this paper is dedicated to studying the sensitivity reach of finding X boson taking realistic experimental situations into account under the effective field theory framework.

This paper is organized as follows: we first set up our theoretical framework and introduce the effective interactions in Section II. The analysis for BESIII is carried out in Section III.

¹ Primordial black holes may explain the whole DM. See, e.g., [5].

In Section IV and V, $e^+e^- \rightarrow \ell^+\ell^- J/\Psi$ and $e^+e^- \rightarrow X + J/\Psi$ with displaced vertex signal are analyzed, respectively for Belle II. Finally, our results are summarized in Section VI.

II. EFFECTIVE LAGRANGIAN

The vectorlike interactions of the X boson with the SM fermions, f , are introduced by the effective Lagrangian:

$$\mathcal{L} \supset -eX_\mu \sum_f \varepsilon_f \bar{f} \gamma^\mu f, \quad (1)$$

where we regard the couplings ε_f as free parameters without knowing the origin. In particular, we will assume four universal couplings, $\varepsilon_u, \varepsilon_d, \varepsilon_e$, and ε_ν , for up-type quarks, down-type quarks, charged leptons, and neutrinos, respectively, in our analysis below. We also note that the new interactions do not induce any axial anomaly by construction.

If the new boson X is responsible for the recent Atomki anomaly [22] via the process ${}^8\text{Be} + X \rightarrow {}^8\text{Be} + e^+e^-$, its mass should be $m_X \simeq 17$ MeV and the couplings with the first generation quarks should be in a particular window [23–25]:

$$|\varepsilon_u + \varepsilon_d| \simeq 3.7 \times 10^{-3}. \quad (2)$$

From the NA48/2 experiment for $\pi^0 \rightarrow X\gamma$, we require a *protophobic* condition [26]:

$$|2\varepsilon_u + \varepsilon_d| < 8 \times 10^{-4}. \quad (3)$$

Taking both relations in Eq. 2 and Eq. 3 into account, we finally get the preferred value for up-type and down-type quark couplings:

$$\varepsilon_u \simeq \pm 3.7 \times 10^{-3}, \quad \varepsilon_d \simeq \mp 7.4 \times 10^{-3}, \quad (4)$$

which we will rely on below.

The coupling to the leptons, especially to electron and electron-neutrino, are stringently constrained by the beam dump experiment SLAC E141 [27], the anomalous magnetic moment of the electron $g - 2$ [28], and neutrino-electron scattering experiment [29]:

$$4.2 \times 10^{-4} \lesssim |\varepsilon_e| \lesssim 1.4 \times 10^{-3}, \quad (5)$$

$$\sqrt{\varepsilon_e \varepsilon_\nu} \lesssim 7 \times 10^{-5}. \quad (6)$$

When a small coupling for neutrino $\varepsilon_\nu \ll 10^{-6}$ is assumed, we do not worry about constraints from neutrinos.

III. SIGNAL AND BACKGROUND FROM $J/\Psi \rightarrow \eta_c e^+ e^-$

In the SM, the decay $J/\Psi \rightarrow \eta_c \gamma^* \rightarrow \eta_c e^+ e^-$ is radiatively allowed [30]. Its partial width is expressed with the form factor $f_{\text{VP}}(0)$ for on-shell photon at the vanishing momentum transfer limit $q^2 = 0$ [31]

$$\Gamma(J/\Psi \rightarrow \eta_c \gamma) = \frac{1}{3} \frac{\alpha_{\text{EM}}(m_{J/\Psi}^2 - m_{\eta_c}^2)^3}{8m_{J/\Psi}^3} |f_{\text{VP}}(0)|^2, \quad (7)$$

from which the form factor $|f_{\text{VP}}(0)| = 0.68949 \text{ GeV}^{-1}$ is determined with the fine structure constant $\alpha_{\text{EM}} \simeq 1/128$, the masses of J/Ψ and η_c , $m_{J/\Psi} = 3.0969 \text{ GeV}$, and $m_{\eta_c} = 2.9839 \text{ GeV}$, respectively, and the measured width $\Gamma(J/\Psi \rightarrow \eta_c \gamma) = 1.5793 \text{ keV}$ [7, 32–34]. The form factor $f_{\text{VP}}(q^2)$ for general $q^2 \neq 0$ is obtained by $F_{\text{VP}}(q^2) \equiv f_{\text{VP}}(q^2)/f_{\text{VP}}(0) = 1/(1 - \frac{q^2}{\Lambda^2})$ from the pole approximation with pole mass $\Lambda = m_{\psi'} = 3.686097 \text{ GeV}$ for J/Ψ .

The normalized differential widths for partial decay widths of $J/\Psi \rightarrow \eta_c \gamma^* \rightarrow \eta_c e^+ e^-$ and $J/\Psi \rightarrow \eta_c X^* \rightarrow \eta_c e^+ e^-$, respectively for off-shell photon and X boson are obtained using a common factor $F_{\text{VP}}(q^2)$ [30]:

$$\begin{aligned} \frac{d\Gamma_{\eta_c \gamma^*}}{dq^2 \Gamma_{J/\Psi \rightarrow \eta_c \gamma}} &= |F_{\text{VP}}(q^2)|^2 \times F_{\text{QED}}(q^2) \\ \frac{d\Gamma_{\eta_c X^*}}{dq^2 \Gamma_{J/\Psi \rightarrow \eta_c \gamma}} &= |F_{\text{VP}}(q^2)|^2 \times F_X(q^2), \end{aligned} \quad (8)$$

where the kinematic window is given as $(2m_e)^2 \leq q^2 = m_{e^+e^-}^2 \leq (m_{J/\Psi} - m_{\eta_c})^2$. Since the mass difference between J/Ψ and η_c is only 113 MeV, it is hard to significantly boost X boson in this channel and produce displaced-vertex signal in a collider detector.

The precise expression for the factor F_{QED} is shown in Ref. [30] where the factor is found to include the amplitude square and phase space factor for off-shell photon. Analogous expression for F_X is obtained:

$$\begin{aligned} F_X(q^2) &= \frac{\alpha_{\text{EM}}(\varepsilon_c \cdot \varepsilon_e)^2}{3\pi} \left(\frac{q^2}{[(q^2 - m_X^2)^2 + m_X^2 \Gamma_X^2]} \right) \\ &\times \left(1 - \frac{4m_e^2}{q^2} \right)^{1/2} \left(1 + \frac{2m_e^2}{q^2} \right) \left[\left(1 + \frac{q^2}{m_{J/\Psi}^2 - m_{\eta_c}^2} \right)^2 - \frac{4m_{J/\Psi}^2 q^2}{(m_{J/\Psi}^2 - m_{\eta_c}^2)^2} \right]^{3/2} \end{aligned} \quad (9)$$

by replacing the couplings and propagator from F_{QED} .

Assuming that $\varepsilon_\nu \ll 10^{-6}$ and $\varepsilon_e \simeq 10^{-3}$, and the quark channels are kinematically forbidden with $m_X \leq 2m_\pi$, the X boson dominantly decay to electrons with the width

$$\Gamma_{X \rightarrow e^+ e^-} = \frac{\varepsilon_e^2 \alpha_{\text{EM}} m_X}{3} \left(1 + \frac{2m_e^2}{m_X^2} \right) \sqrt{1 - \frac{4m_e^2}{m_X^2}}, \quad (10)$$

which is narrow $\Gamma_X \ll m_X$.

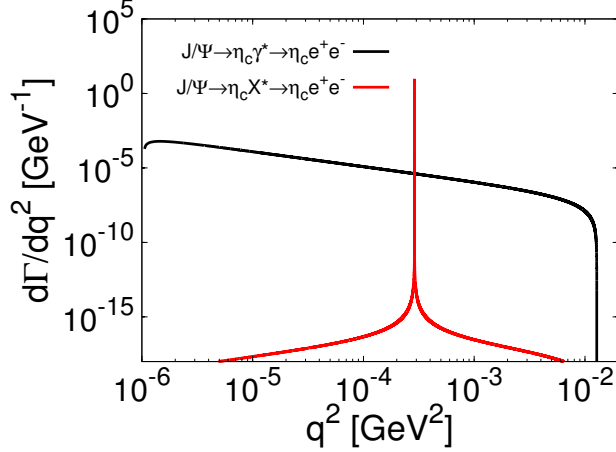


FIG. 1. The e^+e^- invariant mass distributions of signal $J/\Psi \rightarrow \eta_c X^* \rightarrow \eta_c e^+ e^-$ (red) and background $J/\Psi \rightarrow \eta_c \gamma^* \rightarrow \eta_c e^+ e^-$ (black), where $q^2 \equiv m_{e^+e^-}^2$. Input parameters are $m_X = 17$ MeV, $\varepsilon_c = 3.7 \times 10^{-3}$, and $\varepsilon_e = 10^{-3}$.

After performing the integration of q^2 , we can obtain the partial decay width $\Gamma_{\eta_c X^*}$. By inserting favoured coupling values $\varepsilon_c = \varepsilon_u = 3.7 \times 10^{-3}$, $\varepsilon_e = 10^{-3}$ and fixing $m_X = 17$ MeV for ${}^8\text{Be}^*$ anomaly, it gives $\Gamma_{\eta_c \gamma^*} = 2.09 \times 10^{-5}$ keV and implies

$$\text{Br}(J/\Psi \rightarrow \eta_c X^* \rightarrow \eta_c e^+ e^-) = 1.64 \times 10^{-6} \left(\frac{\varepsilon_c}{10^{-2}} \right)^2,$$

which is about three orders of magnitude smaller than that of the $\eta_c \gamma^*$ background, $\text{Br}(J/\Psi \rightarrow \eta_c \gamma^* \rightarrow \eta_c e^+ e^-) = 1.03 \times 10^{-4}$.²

The e^+e^- invariant-mass-squared distributions for signal ($\eta_c X^*$) and background ($\eta_c \gamma^*$) are compared in Fig. 1. The different features are clearly displayed: the signal has a peak at $q^2 = m_X^2$ and the background is broadly distributed. Therefore our task now is to efficiently extract the signal near the peak and suppress the background.

We first impose a kinematic condition for signal: $M_{e^+e^-} \subset [(m_X - \sigma_m), (m_X + \sigma_m)]$, where σ_m is the e^+e^- mass resolution which is roughly of the same order of magnitude as the energy resolution σ_E . The signal yield S and background yield B are now obtained as

$$\begin{aligned} S &= N_{J/\Psi} \times \frac{\int_{(m_X - \sigma_m)^2}^{(m_X + \sigma_m)^2} dq^2 \frac{d\Gamma_{\eta_c X^*}}{dq^2}}{\Gamma_{J/\Psi}}, \\ B &= N_{J/\Psi} \times \frac{\int_{(m_X - \sigma_m)^2}^{(m_X + \sigma_m)^2} dq^2 \frac{d\Gamma_{\eta_c \gamma^*}}{dq^2}}{\Gamma_{J/\Psi}}, \end{aligned} \quad (11)$$

where $N_{J/\Psi}$ is the total number of J/Ψ produced in the collision, and $\Gamma_{J/\Psi} = 92.9$ keV is the total decay width of J/Ψ [7].

² In the background estimation, the other background sources are not considered. For instance, $\gamma \rightarrow e^+e^-$ conversion near the detector materials is contributed with $J/\Psi \rightarrow \eta_c \gamma$ decay as a background source. The process is suppressed by examining the vertex position of the resulting e^+e^- . For the vertexing performance of Belle II, the reader is directed to Ref. [35].

TABLE I. The branching fractions of η_c decay modes with corresponding efficiencies.

Branching Ratio	Detection efficiency
$\text{Br}(\eta_c \rightarrow K^+ K^- \pi^0) = (1.15 \pm 0.12)\%$	18.82%
$\text{Br}(\eta_c \rightarrow K_S^0 K^\pm \pi^\mp) = (2.60 \pm 0.21)\%$	21.22%
$\text{Br}(\eta_c \rightarrow 2(\pi^+ \pi^- \pi^0)) = (15.2 \pm 1.8)\%$	3.07%

The BESIII experiment, which has collected 10^{10} J/Ψ events in the resonance process $e^+e^- \rightarrow J/\Psi$ [30], plans to increase the size of J/Ψ sample to 10^{11} events in the near future. The energy resolution of BESIII is $\sigma_E/E \simeq 0.005$ for the final-state electron, which smears the invariant mass distribution of e^+e^- by $\sigma_m \simeq 1$ MeV.

In order to exclusively reconstruct the $J/\Psi \rightarrow \eta_c e^+e^-$ decays, we have to consider η_c decay modes that can be fully reconstructed with reasonable background contamination. Table I lists the branching fractions of a few such η_c decay modes along with the corresponding efficiencies [36].

The overall efficiency ϵ of the above three η_c modes is obtained by adding the individual efficiencies weighted by their corresponding branching fractions: $\epsilon = 1.23\%$. Given these, and taking 17 MeV X boson for ${}^8\text{Be}^*$ anomaly to be real, we list, in Table II, the expected significances of $J/\Psi \rightarrow \eta_c X \rightarrow \eta_c e^+e^-$ with $N_{J/\Psi} = 10^{11}$ at BESIII under the assumption of $\epsilon_c = \epsilon_u$, for various σ_m values.

TABLE II. For $N_{J/\Psi} = 10^{11}$ and favoured parameters $\epsilon_c = \epsilon_u = 3.7 \times 10^{-3}$, $\epsilon_e = 10^{-3}$, $m_X = 17$ MeV for ${}^8\text{Be}^*$ anomaly, the significances of signal to background from $J/\Psi \rightarrow \eta_c e^+e^-$ with various energy resolutions of detector and 1.23% η_c reconstruction efficiency.

	$\sigma_m=1$ MeV	$\sigma_m=2$ MeV	$\sigma_m=5$ MeV	$\sigma_m=10$ MeV	$\sigma_m=15$ MeV
S	188	263	277	277	277
B	3686	7399	18989	42436	87640
S/\sqrt{B}	3.10	3.06	2.01	1.34	0.94

For general light vector boson searches through $J/\Psi \rightarrow \eta_c e^+e^-$, the variation of the expected significance over $(m_X, \epsilon_c, \epsilon_e)$ are shown in Fig. 2. With the present value of $N_{J/\Psi} = 10^{10}$ at BESIII, the region of sensitivity is $|\epsilon_c| \gtrsim 5 \times 10^{-3}$ at $m_X \simeq 17$ MeV as shown in the upper left panel of Fig. 2 and left panel of Fig. 3. The sensitivity slightly improves as m_X increases, because of the reduction of background (see Fig. 1), and reaches the maximal sensitivity $|\epsilon_c| \gtrsim 3 \times 10^{-3}$ at $m_X \simeq 60$ MeV. But as m_X approaches $m_{J/\Psi} - m_{\eta_c}$, the sensitivity becomes weaker due to the phase space suppression. The two right panels of Fig. 2 show that the significance is independent of the ϵ_e as we expect from the narrow width approximation. For $N_{J/\Psi} = 10^{11}$ which is expected in the near future, the projected sensitivity becomes $|\epsilon_c| \gtrsim 3 \times 10^{-3}$ at $m_X \simeq 17$ MeV as shown in the bottom-left panel of

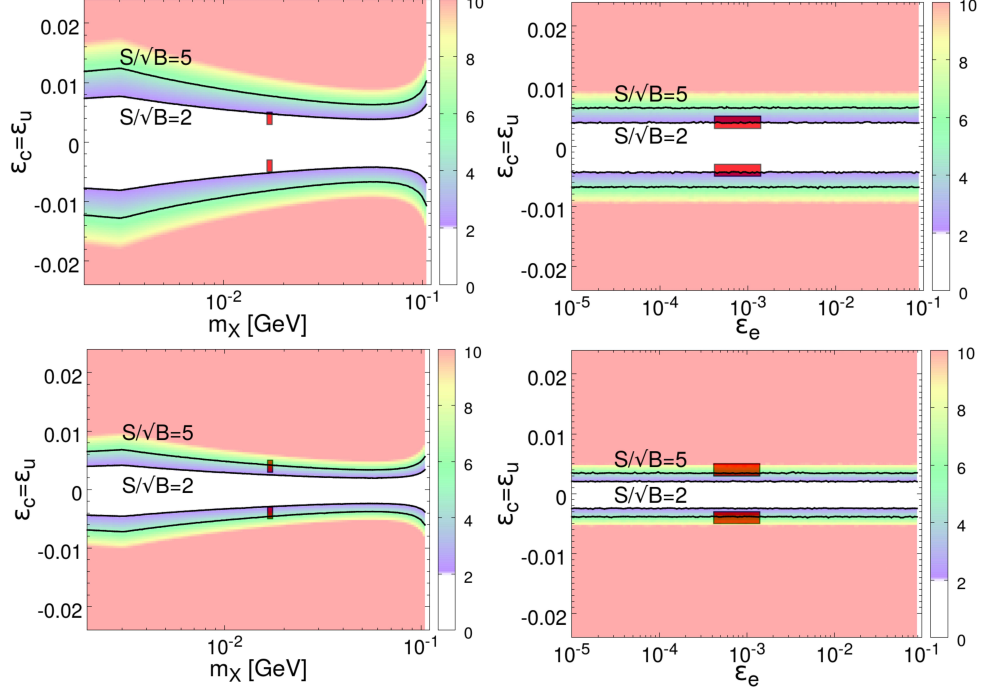


FIG. 2. The significance S/\sqrt{B} on (m_X, ε_c) and $(\varepsilon_c, \varepsilon_e)$ planes from $J/\Psi \rightarrow \eta_c e^+ e^-$ light X vector boson searches at BESIII. Adopt $N_{J/\Psi} = 10^{10}$ (upper panels) and $N_{J/\Psi} = 10^{11}$ (bottom panels), reconstructed efficiency of η_c from Table I, and the invariant mass cut $|M_{ee} - m_X| \leq \sigma_m = 2$ MeV. The red boxes indicate the preferred regions for ${}^8\text{Be}^*$ anomaly.

Fig. 2 and the right panel of Fig. 3, whereby the entire favored region of ${}^8\text{Be}^*$ anomaly can be probed.

An alternative way to explicitly reconstructing η_c in $J/\Psi \rightarrow \eta_c e^+ e^-$ at BESIII is to use the recoil of $e^+ e^-$. As the e^\pm carries low energy around 50 MeV, it gets difficult to distinguish

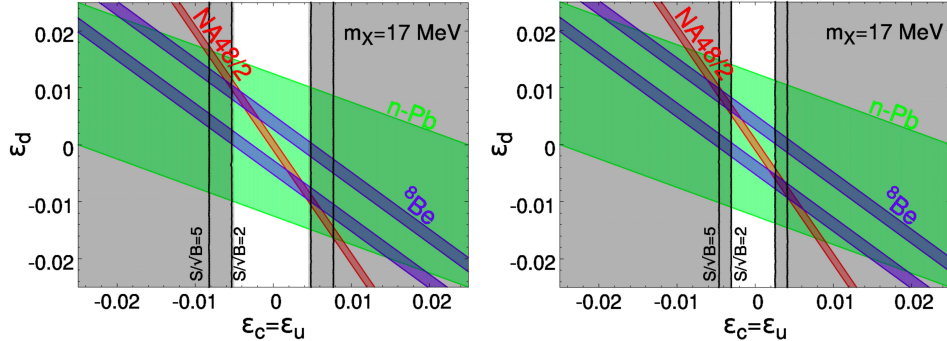


FIG. 3. The current (left-panel: $N_{J/\Psi} = 10^{10}$) and future (right-panel: $N_{J/\Psi} = 10^{11}$) BESIII sensitivities by assuming the reconstruction efficiencies from Table I and taking the invariant mass cut $|M_{ee} - m_X| \leq \sigma_m = 2$ MeV. Compare with the allowed regions for ${}^8\text{Be}^*$ anomaly, NA48/2 for π^0 decay [26] and neutron-nucleus scattering [37].

e^\pm tracks from π^\pm background. With an improvement of low-energy electron identification in the future, the BESIII with $N_{J/\Psi} = 10^{11}$ can reach the sensitivity of $|\varepsilon_c| \simeq 10^{-3}$.

IV. THE $e^+e^- \rightarrow \ell^+\ell^- + J/\Psi \rightarrow \ell^+\ell^-e^+e^-\eta_c$ AT BELLE II

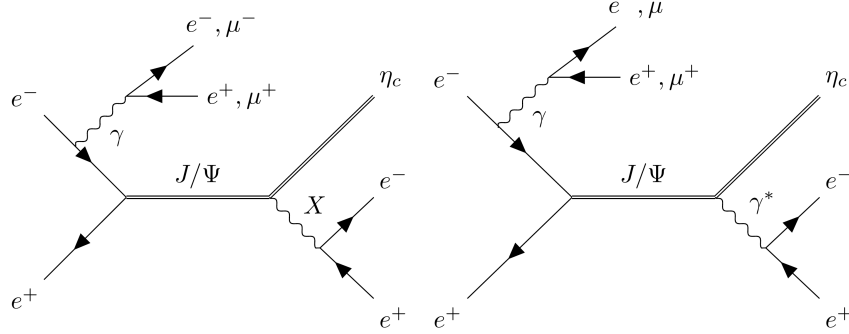


FIG. 4. The feynman diagrams of the signal (left) and background (right)

For vector meson J/Ψ , the partial width to e^+e^- is given by

$$\Gamma_{J/\Psi \rightarrow e^+e^-} = \frac{g_{J/\Psi ee}^2}{12\pi} m_{J/\Psi} \left(1 + \frac{2m_e^2}{m_{J/\Psi}^2} \right) \sqrt{1 - \frac{4m_e^2}{m_{J/\Psi}^2}}, \quad (12)$$

where $g_{J/\Psi ee} = 8.2048 \times 10^{-3}$ [7] is the coupling strength in the effective interaction $g_{J/\Psi ee} [\bar{e}\gamma^\mu e](J/\Psi)_\mu$ that matches the measured value $\Gamma_{J/\Psi \rightarrow e^+e^-} = 5.53$ keV [7].

Then the cross sections to $\ell^+\ell^-J/\Psi$ where $\ell = e, \text{ or } \mu$ at Belle II are obtained via $e^+e^- \rightarrow \gamma^*J/\Psi$:

$$\begin{aligned} \sigma(e^+e^- \rightarrow \gamma^* + J/\Psi \rightarrow e^+e^-J/\Psi) &= 286 \text{ fb}, \\ \sigma(e^+e^- \rightarrow \gamma^* + J/\Psi \rightarrow \mu^+\mu^-J/\Psi) &= 58.4 \text{ fb}. \end{aligned} \quad (13)$$

With the design integrated luminosity $\mathcal{L} = 50 \text{ ab}^{-1}$, we estimate $N_{J/\Psi} = 1.75 \times 10^7$ events for $e^+e^- \rightarrow \gamma^* + J/\Psi \rightarrow \ell^+\ell^-J/\Psi$ at Belle II. This $N_{J/\Psi}$ is applied to Eq. 11, along with Eq. 12, to give estimates of S and B :

$$\begin{aligned} S &= \mathcal{L} \times \sigma(e^+e^- \rightarrow \ell^+\ell^-J/\Psi) \times \text{Br}(J/\Psi \rightarrow \eta_c X^* \rightarrow \eta_c e^+e^-) \simeq 28.2 \left(\frac{\varepsilon_c}{10^{-2}} \right)^2, \\ B &= \mathcal{L} \times \sigma(e^+e^- \rightarrow \ell^+\ell^-J/\Psi) \times \text{Br}(J/\Psi \rightarrow \eta_c \gamma^* \rightarrow \eta_c e^+e^-) \simeq 1772. \end{aligned} \quad (14)$$

Therefore, the estimated S/\sqrt{B} is too small at this level so that we will improve the analysis by a more realistic MC study below.

For event generation, we use MG5_AMC@NLO [38] for both signal and background with FEYNRULES v2.0 [39] model for $J/\Psi, \eta_c$ mesons and X boson couplings and X couples to

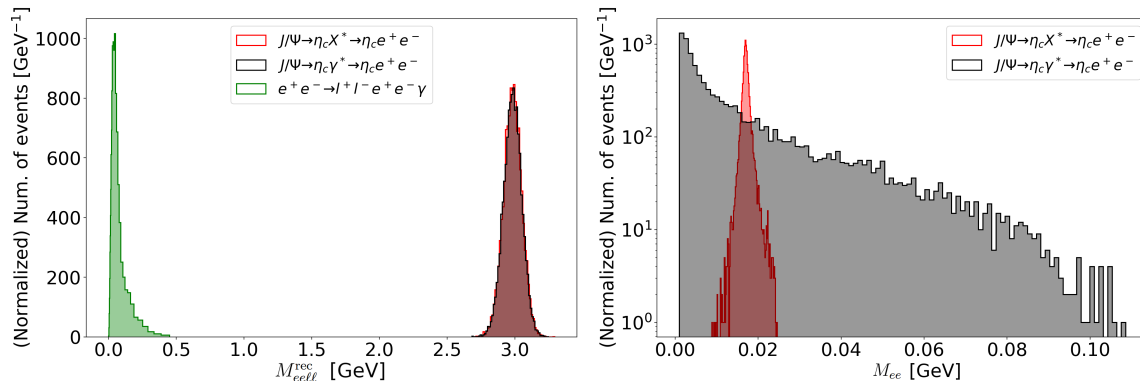


FIG. 5. The $e^+e^-\ell^+\ell^-$ recoil mass (left) and e^+e^- invariant mass (right) distributions for the parton level Monte-Carlo simulation data with the smearing effect. Input parameter is $m_X = 17$ MeV. Here, we normalized to 10^5 events for each channel.

the leptons. We generate with the $E_{\text{beam}1,2} = 5.2941$ GeV in the CM frame, which is boosted by $\beta = 0.2732$ with respect to the lab frame. The amplitude of the electromagnetic Dalitz decay, $V \rightarrow Pe^+e^-$ can be written in a Lorentz-invariant form [30],

$$T(V \rightarrow Pe^+e^-) = 4\pi\alpha_{\text{EM}}f_{\text{VP}}\epsilon^{\mu\nu\rho\sigma}p_\mu q_\nu \epsilon_\rho \frac{1}{q^2}\bar{u}_1\gamma_\sigma\nu_2 \quad (15)$$

and we can obtain the interaction Lagrangian as,

$$\mathcal{L} \supset f_{\text{VP}}(-2\sqrt{\pi\alpha_{\text{EM}}}\partial_\mu P\partial_\nu V_\rho\epsilon^{\mu\nu\rho\sigma}A_\sigma - g_{Xc}\partial_\mu P\partial_\nu V_\rho\epsilon^{\mu\nu\rho\sigma}X_\sigma) - g_{eV}\bar{e}\gamma^\mu eV_\mu - g_{Xe}\bar{e}\gamma^\mu eX_\mu, \quad (16)$$

where g_{Xc} , g_{Xe} , and g_{eV} are the effective coupling constants, whose numerical values are to be obtained by experiments.

Similar to the BESIII, photon conversion process where the photon from $J/\Psi \rightarrow \eta_c\gamma$ hits the beam pipe or vertex detector layers and converts to e^+e^- can be a background source, but they are controlled by examining the e^+e^- vertex position. Another possible background is $e^+e^- \rightarrow \ell^+\ell^- + (\text{anything})$ where (anything) may contain a number of low-momentum charged particles that are misidentified as electrons. However, this process does not show peak in the $M_{\ell^+\ell^-}^{\text{recoil}} \simeq M_{J/\Psi}$ variable, and can be suppressed by inspecting the $M_{\ell^+\ell^-}^{\text{recoil}}$ distribution. In the Fig. 5, the recoil mass of $e^+e^-\ell^+\ell^-$ and invariant mass distributions of e^+e^- are plotted for the signal (shown in red), and the $\ell^+\ell^-e^+e^-(\gamma)$ (green) and $J/\Psi \rightarrow \eta_c\gamma^*$ (gray) backgrounds, where we produce equal number of events ($= 10^5$) for each sample at the parton level before applying any selection cuts. We give a Gaussian smearing effect with the momentum resolution $\sigma_{p_{\ell^\pm}}/p_{\ell^\pm} = 0.005$ on the parton level data for our analysis. To simulate the effects of the Belle II detector, we apply the following baseline cuts: $|\eta_{\ell^\pm}^*| \leq 1.60$ in the CM frame [14, 40], $|E_{\mu^\pm}| \geq 0.6$ GeV, and $|E_{e^\pm}| \geq 0.06$ GeV in the lab frame [41]. Note that we require very low energy threshold for electrons so as to keep most of the signals, because the e^+e^- from $J/\Psi \rightarrow \eta_c e^+e^-$ are very soft. This inevitably

TABLE III. Signal and background events of $e^+e^- \rightarrow \ell^+\ell^-e^+e^-\eta_c$ after cuts at Belle II.

Cuts	B	S
Processes	$\eta_c\gamma^* \rightarrow \eta_c ee$	$\eta_c X \rightarrow \eta_c ee$
	100000	100000
Baseline Cuts	7170	6290
$ M_{e\ell\ell}^{\text{rec}} - m_{\eta_c} \leq 200$ MeV	7071	6219
$ M_{ee} - m_X \leq 2$ MeV	377	5880

would cause large background from pion tracks being misidentified as electrons.³

And we give two kinematic requirements: For the energy-momentum 4-vector of η_c , we use the energy and momentum recoiling against $e^+e^-\ell^+\ell^-$. The signal and background distributions of the recoil mass $M_{e\ell\ell}^{\text{rec}}$, smeared by the charged-track momentum resolution, are displayed in the left panel of Fig. 5. The $J/\Psi \rightarrow \eta_c e^+e^-$ events clearly show a peak at $M_{e\ell\ell}^{\text{rec}} \simeq m_{\eta_c}$, while the $\ell^+\ell^-e^+e^-(\gamma)$ background is mostly populated at $M_{e\ell\ell}^{\text{rec}} \simeq 0$, therefore we require $|M_{e\ell\ell}^{\text{rec}} - m_{\eta_c}| \leq 200$ MeV to eliminate the $\ell^+\ell^-e^+e^-(\gamma)$ background. In addition, we apply $|M_{ee} - m_X| \leq 2$ MeV, whereby the $\eta_c\gamma^*$ background from the process shown in the right panel of Fig. 4 are suppressed. In Table III, we summarize the cumulative effects of the baseline cuts and the kinematic requirements.

The sensitivities of $\ell^+\ell^-e^+e^-$ search at Belle II are derived from the requirement of $S/\sqrt{B} = 2$. Combining Eq. (14) and Table III, we obtain the corresponding values of ε_c with respect to luminosities of 50, 100, and 200 ab^{-1} in Table IV. They are about 5 times larger than the estimates from current BESIII sensitivity $|\varepsilon_c| \gtrsim 5 \times 10^{-3}$ in Section III.

TABLE IV. Sensitivities on ε_c of 17 MeV X boson from $\ell^+\ell^-J/\Psi \rightarrow \ell^+\ell^-e^+e^-\eta_c$ search at Belle II with luminosities 50, 100, and 200 ab^{-1} . Here we require $S/\sqrt{B} = 2$.

Luminosity	50 ab^{-1}	100 ab^{-1}	200 ab^{-1}
$ \varepsilon_c $	$\gtrsim 1.76 \times 10^{-2}$	$\gtrsim 1.48 \times 10^{-2}$	$\gtrsim 1.24 \times 10^{-2}$

V. THE $e^+e^- \rightarrow X + J/\Psi \rightarrow e^+e^- + J/\Psi$ DISPLACED VERTEX AT BELLE II

The X boson produced in the process $e^+e^- \rightarrow X + J/\Psi$ travels several millimeters before decaying into e^+e^- in the Belle II detector and leaves displaced vertex. In particular, when the distance of the flight is between 2 mm and 8 mm, which is inside the beam pipe, and

³ Currently, the most powerful observable for electron identification (e -ID) at Belle II is the E/p where E is the energy measured in the electromagnetic calorimeter and p is the magnitude of 3-momentum measured in the drift chamber. [42] With low-momentum tracks that cannot reach the calorimeter [43], the performance of e -ID will thus degrade. For the actual data analysis, we encourage the Belle II collaboration to improve e -ID for low-momentum tracks along with systematic uncertainties.

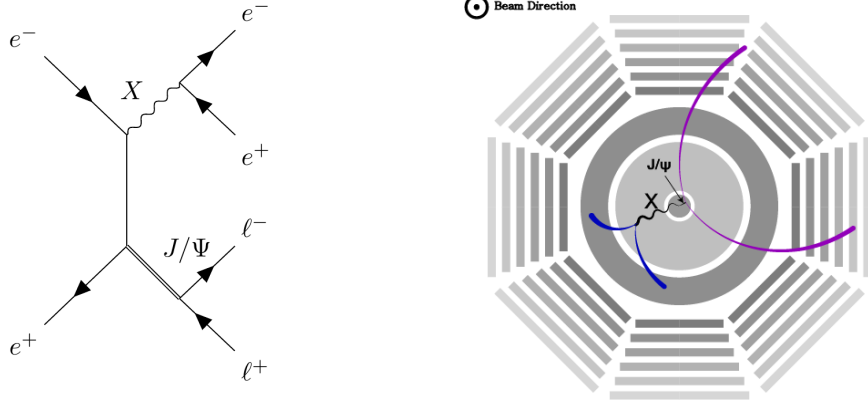


FIG. 6. **(Left Panel)** The Feynman diagram of the $e^+e^- \rightarrow X + J/\Psi \rightarrow e^+e^-\ell^+\ell^-$ signal **(Right Panel)** The schematic picture of the decay process of the long-lived X boson in the Belle II detector.

outside the interaction region, Belle II has excellent power to reconstruct the displaced vertex and makes the signal almost free from the SM background [44]. Therefore, we propose to use the clean displaced e^+e^- vertex from the X boson decay (along with prompt $\ell^+\ell^-$ from J/Ψ).

The leading-order Feynman diagram of the relevant process is shown in the left panel of Fig. 6. A typical event with displaced vertex at Belle II detector with the $\ell^+\ell^-$ from J/Ψ decay is schematically shown in the right panel of Fig. 6.

We note that compared with other lighter vector mesons, the heavier mass of J/Ψ helps to induce larger scattering angle in such a way that more events from $X \rightarrow e^+e^-$ will satisfy the cut $|\eta_{\ell^\pm}^*| \leq 1.60$. Furthermore, the electron and positron from $X \rightarrow e^+e^-$ carry energy above GeV, which make them easier to be distinguished from charged-pion backgrounds.

The other advantage of this channel is that the signal strength only depends on the ε_e coupling since only X - e^+e^- vertices are involved at tree level. For $0.3 \times 10^{-3} \leq \varepsilon_e \leq 0.8 \times 10^{-3}$, it yields a few mm transverse flight distance d_{xy} which is defined as the distance between the beam axis and the X decay vertex. The left-panel of Fig. 7 shows the distribution of d_{xy} corresponding to several values of ε_e .

With the baseline cuts and $2 \text{ mm} \leq d_{xy} \leq 8 \text{ mm}$, we estimate the signal sensitivity by considering two cases: (i) explicitly reconstructing $J/\Psi \rightarrow \ell^+\ell^-$ ($e^+e^-\ell^+\ell^-$ channel'), and (ii) using the recoil mass of $X \rightarrow e^+e^-$ to infer J/Ψ (e^+e^- channel'). Tables V and VI show, respectively for the $e^+e^-\ell^+\ell^-$ and e^+e^- channels, the signal efficiencies and expected significances for various assumed values of ε_e , according to the 50 ab^{-1} luminosity at Belle II and the $e^+e^- \rightarrow X + J/\Psi$ cross section

$$\sigma(e^+e^- \rightarrow X + J/\Psi) = 2.77 \times 10^{-2} \times \left(\frac{\varepsilon_e}{10^{-3}}\right)^2 \text{ fb.} \quad (17)$$

The significances are calculated from the expected p -value of background-only hypothesis for each case.

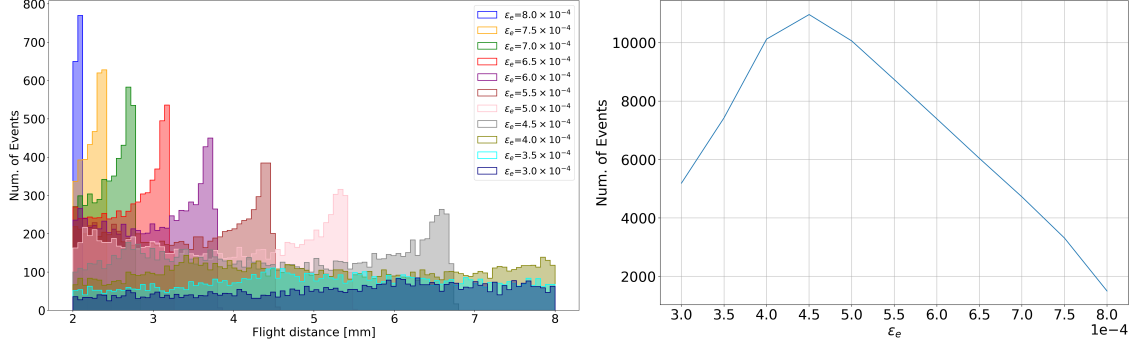


FIG. 7. (Left panel) The transverse flight distance d_{xy} of 17 MeV X boson for ε_e in 0.5×10^{-4} steps from 3×10^{-4} to 8×10^{-4} ; (Right panel) The number of events that pass the baseline cuts and satisfy $2 \text{ mm} \leq d_{xy} \leq 8 \text{ mm}$ from the sample of 10^5 generated signal events.

TABLE V. (From top rows to bottom) The fraction of events (in %) that survive the baseline cuts mentioned in Section.IV, and the flight distance $2 \text{ mm} \leq d_{xy} \leq 8 \text{ mm}$ cuts, for several values of ε_e of 17 MeV X boson; the number of signal events N_S in the $e^+e^-\ell^+\ell^-$ channel at Belle II with 50 ab^{-1} luminosity; and the expected significances assuming 1 event, and 0.1 event of the SM background in the analysis channel after all cuts.

$\varepsilon_e/10^{-4}$	8.0	7.0	6.0	5.0	4.5	4.0	3.0
Baseline Cuts(%)	13.8	13.8	13.8	13.8	13.8	13.8	13.8
$2\text{mm} < d_{xy} < 8\text{mm}$ (%)	1.5	4.7	7.4	10.1	11.0	10.1	5.2
N_S	1.60	3.85	4.42	4.18	3.69	2.69	0.78
Significance ($B = 0.1$)	2.4σ	4.6σ	5.0σ	4.8σ	4.5σ	3.6σ	1.5σ
Significance ($B = 1$)	1.6σ	2.9σ	3.2σ	3.1σ	2.8σ	2.3σ	1.2σ

TABLE VI. The same as Table V, but using the e^+e^- channel

$\varepsilon_e/10^{-4}$	8.0	7.0	5.0	4.0	3.0	2.0	1.0
Baseline Cuts(%)	17.6	17.6	17.6	17.6	17.6	17.6	17.6
$2\text{mm} < d_{xy} < 8\text{mm}$ (%)	1.6	5.3	12.3	12.9	7.4	2.3	0.5
N_S	14.6	35.7	42.7	28.7	9.23	1.28	0.07
Significance ($B = 0.1$)	$> 5\sigma$					2.2σ	0.4σ
Significance ($B = 1$)	$> 5\sigma$					1.6σ	0.9σ

The final result of expected sensitivity with Belle II at 50 ab^{-1} luminosity is shown in Fig. 8. Also displayed in Fig. 8 are the expected results with the η_c -related studies at Belle II and BESIII as discussed in Sections III and IV. The displaced e^+e^- vertex searches

can probe the 17 MeV X boson in the region

$$2.5 \times 10^{-4} \leq \varepsilon_e \leq 8.0 \times 10^{-4}$$

with significance larger than 2 by assuming near-zero background, and it covers the ε_e region preferred by Atomki. While we expect less than one signal event with the currently available Belle data sample of 1 ab^{-1} , we can start exploring the Atomki preferred region within a few years once Belle II accumulates data sample of 10 ab^{-1} or more.

Our study with the displaced vertex is extended for wider mass range of X -like boson, whereby we determine the region of sensitivity with Belle II at 50 ab^{-1} , as displayed in Fig. 8. Two cases are considered: $B = 0.1$ and $B = 1$, where B is the expected number of background events from the SM processes. We then use the Poisson probability of the expected background to fluctuate upward, to calculate the p -values and the corresponding significances. The 2σ significance region with $B = 0.1$ ($B = 1$) is shown as the yellow (green)

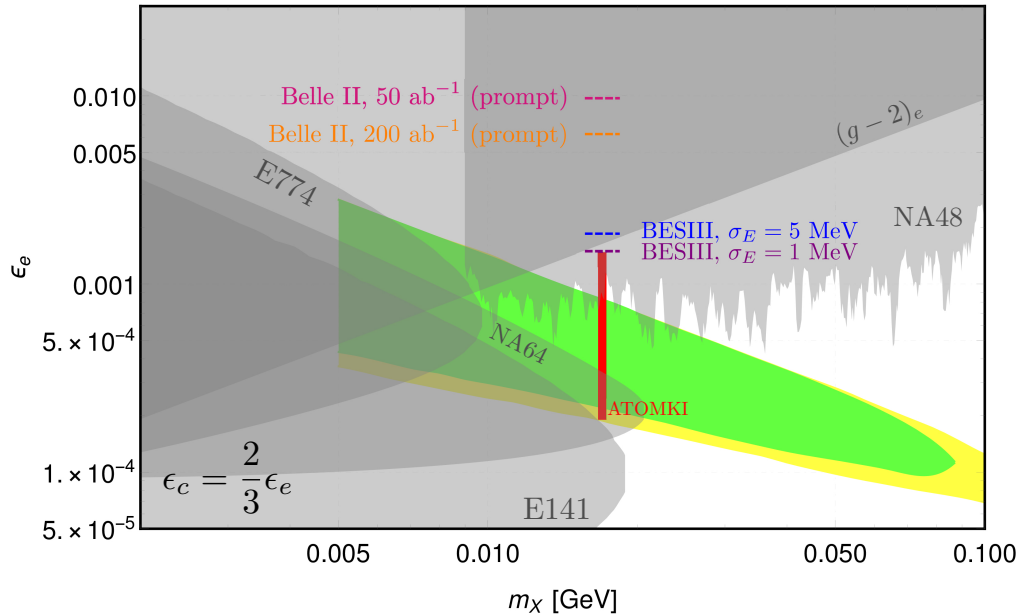


FIG. 8. The yellow (green) contour corresponds $\geq 2\sigma$ significance assuming SM background $B = 0.1$ ($B = 1$) from e^+e^- channel at Belle II with 50 ab^{-1} luminosity, which probes rest of the favour parameter region of Atomki (red vertical band). The gray-shaded regions are excluded by current experiments relate to Xee coupling. Compare to the sensitivities of $e^+e^- \rightarrow \ell^+\ell^- + J/\Psi \rightarrow \ell^+\ell^-e^+e^-\eta_c$ channel at Belle II and $e^+e^- \rightarrow J/\Psi \rightarrow e^+e^-\eta_c$ channel at BESIII by assuming the kinematic mixing between X boson and photon, bringing the relation $\varepsilon_c = \frac{2}{3}\varepsilon_e$. For the future Belle II experiments $50, 200 \text{ ab}^{-1}$ in the 17 MeV mass region, the significance bounds are denoted by magenta, orange dotted lines, respectively. In the case of BESIII for the energy resolutions $\sigma_E = 1 \text{ MeV}$ and 5 MeV , corresponding to section III, they are denoted in purple and blue, respectively.

contour in Fig. 8, which yields signal event $N_S \simeq 1$ ($N_S \simeq 2$)⁴. This study can probe the parameter region of $5 \text{ MeV} \leq m_X \leq 100 \text{ MeV}$ and $1.0 \times 10^{-4} \leq \varepsilon_e \leq 3 \times 10^{-3}$, which have not been constrained by any existing experiments. The upper edge of this region is determined by the condition $2 \text{ mm} \leq d_{xy}$, while the lower edge is limited by the statistics. Therefore, with even higher luminosity of Belle II exceeding the target 50 ab^{-1} , the lower edge of the sensitivity region can be extended further.

VI. SUMMARY AND CONCLUSION

In summary, we propose several studies using J/Ψ at lepton colliders such as Belle II and BESIII, to search for light vector boson around the mass range suggested by the ${}^8\text{Be}^*$ anomaly of the ATOMKI experiment. At BESIII, the $J/\Psi \rightarrow \eta_c X \rightarrow \eta_c e^+ e^-$ channel can be used to constrain the vector boson and charm quark coupling, ε_c . With the currently available sample of $N_{J/\Psi} = 10^{10}$ and effective η_c reconstruction efficiency of 1.23%, we can exclude the region $|\varepsilon_c| \gtrsim 5 \times 10^{-3}$ for $m_X = 17 \text{ MeV}$. If $N_{J/\Psi} = 10^{11}$ is produced at BESIII in the near future, exclusion of the region $|\varepsilon_c| \simeq 3 \times 10^{-3}$ might be achieved. If universal coupling to up-type quarks is assumed, we expect that the entire favored signal region from the ${}^8\text{Be}^*$ anomaly could be covered.

On the other hand at Belle II, with higher CM energy of 10.59 GeV, we propose to study the process $e^+ e^- \rightarrow \ell^+ \ell^- J/\Psi$ followed by $J/\Psi \rightarrow \eta_c X \rightarrow \eta_c e^+ e^-$. Using the recoil mass against $\ell^+ \ell^- e^+ e^-$, we perform MC study and find that the expected production of J/Ψ events is about three orders of magnitude smaller than that of BESIII, thus yielding the sensitivity of $|\varepsilon_c| \gtrsim 1.8 \times 10^{-2}$ at $m_X = 17 \text{ MeV}$.

Alternatively, we can study the process $e^+ e^- \rightarrow X + J/\Psi \rightarrow e^+ e^- \ell^+ \ell^-$ at Belle II and directly constrain the X boson-electron coupling. The X boson is boosted by the higher CM energy and heavy mass of J/Ψ , producing displaced vertex of $X \rightarrow e^+ e^-$ which is longer than several millimeters. Particularly, it is almost background free when the transverse flight distance is $2 \text{ mm} \leq d_{xy} \leq 8 \text{ mm}$. Selecting this window and requiring $> 2\sigma$ significance, it gives the sensitivity $2.0 \times 10^{-4} \leq |\varepsilon_e| \leq 8.0 \times 10^{-4}$ at $m_X = 17 \text{ MeV}$ for 50 ab^{-1} luminosity and covers most of the favored signal region from the claimed ${}^8\text{Be}^*$ anomaly. Extending the range of the X boson mass, this method can cover the unprecedented parameter space of $9 \text{ MeV} \leq m_X \leq 100 \text{ MeV}$ and $1.0 \times 10^{-4} \leq |\varepsilon_e| \leq 10^{-3}$.

⁴ In this case, the p -value is obtained as $\sum_{n \geq N_S + B} P(n|B)$ which is the probability of upward fluctuation based on the SM-only hypothesis with $P(n|B)$ being the Poisson probability of observing n events given B events of expected background. Then the confidence level (CL) is $\text{CL} = 1 - p$. The 2σ significance corresponds to 95.4% CL. For $B = 1$ (0.1) events, we need $N_S \simeq 2$ (1) signal events to attain 2σ significance.

ACKNOWLEDGMENTS

The work is supported in part by the National Research Foundation of Korea [NRF-2018R1A4A1025334 (SCP, YJK), NRF-2019R1A2C1089334 (SCP), and NRF-2020R1I1A1A01066413 (PYT)].

-
- [1] SUPER-KAMIOKANDE collaboration, Y. Fukuda et al., *Evidence for oscillation of atmospheric neutrinos*, *Phys. Rev. Lett.* **81** (1998) 1562–1567, [[hep-ex/9807003](#)].
 - [2] MUON G-2 collaboration, G. Bennett et al., *Final Report of the Muon E821 Anomalous Magnetic Moment Measurement at BNL*, *Phys. Rev. D* **73** (2006) 072003, [[hep-ex/0602035](#)].
 - [3] A. Keshavarzi, D. Nomura and T. Teubner, *$g - 2$ of charged leptons, $\alpha(M_Z^2)$, and the hyperfine splitting of muonium*, *Phys. Rev. D* **101** (2020) 014029, [[1911.00367](#)].
 - [4] PLANCK collaboration, N. Aghanim et al., *Planck 2018 results. VI. Cosmological parameters*, *Astron. Astrophys.* **641** (2020) A6, [[1807.06209](#)].
 - [5] D. Y. Cheong, S. M. Lee and S. C. Park, *Primordial Black Holes in Higgs- R^2 Inflation as a Whole Dark Matter*, [1912.12032](#).
 - [6] L. Canetti, M. Drewes and M. Shaposhnikov, *Matter and Antimatter in the Universe*, *New J. Phys.* **14** (2012) 095012, [[1204.4186](#)].
 - [7] PARTICLE DATA GROUP collaboration, P. Zyla et al., *Review of Particle Physics*, *PTEP* **2020** (2020) 083C01.
 - [8] X.-G. He, G. C. Joshi, H. Lew and R. Volkas, *Simplest Z-prime model*, *Phys. Rev. D* **44** (1991) 2118–2132.
 - [9] W. Altmannshofer, S. Gori, S. Profumo and F. S. Queiroz, *Explaining dark matter and B decay anomalies with an $L_\mu - L_\tau$ model*, *JHEP* **12** (2016) 106, [[1609.04026](#)].
 - [10] P. Foldenauer, *Light dark matter in a gauged $U(1)_{L_\mu - L_\tau}$ model*, *Phys. Rev. D* **99** (2019) 035007, [[1808.03647](#)].
 - [11] S. Baek, N. Deshpande, X. He and P. Ko, *Muon anomalous $g-2$ and gauged $L(\text{muon}) - L(\text{tau})$ models*, *Phys. Rev. D* **64** (2001) 055006, [[hep-ph/0104141](#)].
 - [12] Y. Kaneta and T. Shimomura, *On the possibility of a search for the $L_\mu - L_\tau$ gauge boson at Belle-II and neutrino beam experiments*, *PTEP* **2017** (2017) 053B04, [[1701.00156](#)].
 - [13] T. Araki, S. Hoshino, T. Ota, J. Sato and T. Shimomura, *Detecting the $L_\mu - L_\tau$ gauge boson at Belle II*, *Phys. Rev. D* **95** (2017) 055006, [[1702.01497](#)].
 - [14] Y. Jho, Y. Kwon, S. C. Park and P.-Y. Tseng, *Search for muon-philic new light gauge boson at Belle II*, *JHEP* **10** (2019) 168, [[1904.13053](#)].
 - [15] A. Berlin, D. Hooper, G. Krnjaic and S. D. McDermott, *Severely Constraining Dark Matter Interpretations of the 21-cm Anomaly*, *Phys. Rev. Lett.* **121** (2018) 011102, [[1803.02804](#)].

- [16] W. Altmannshofer, S. Gori, M. Pospelov and I. Yavin, *Quark flavor transitions in $L_\mu - L_\tau$ models*, *Phys. Rev. D* **89** (2014) 095033, [1403.1269].
- [17] S. Shinohara, “Search for the rare decay $K_L \rightarrow \pi^0 \nu \bar{\nu}$ at J-PARC KOTO experiment.” KAON2019, Perugia, Italy, 10-13 Sep, 2019.
- [18] Y.-C. Tung, “Recent Results from KOTO Experiment.” PIC2019, Taipei, Taiwan, 16-20 Sep, 2019.
- [19] C. Lin, “Recent Result on the Measurement of $K_L \rightarrow \pi^0 \nu \bar{\nu}$ at the J-PARC KOTO Experiment.” The 3rd J-PARC Symposium, Tsukuba, Japan, 23-26 Sep, 2019.
- [20] Y. Jho, S. M. Lee, S. C. Park, Y. Park and P.-Y. Tseng, *Light gauge boson interpretation for $(g - 2)_\mu$ and the $K_L \rightarrow \pi^0 + (\text{invisible})$ anomaly at the J-PARC KOTO experiment*, *JHEP* **04** (2020) 086, [2001.06572].
- [21] A. J. Krasznahorkay et al., *Observation of Anomalous Internal Pair Creation in $Be8$: A Possible Indication of a Light, Neutral Boson*, *Phys. Rev. Lett.* **116** (2016) 042501, [1504.01527].
- [22] A. Krasznahorkay et al., *New evidence supporting the existence of the hypothetical $X17$ particle*, 1910.10459.
- [23] J. L. Feng, B. Fornal, I. Galon, S. Gardner, J. Smolinsky, T. M. P. Tait et al., *Protophobic Fifth-Force Interpretation of the Observed Anomaly in 8Be Nuclear Transitions*, *Phys. Rev. Lett.* **117** (2016) 071803, [1604.07411].
- [24] B. Fornal, *Is There a Sign of New Physics in Beryllium Transitions?*, *Int. J. Mod. Phys. A* **32** (2017) 1730020, [1707.09749].
- [25] J. L. Feng, T. M. Tait and C. B. Verhaaren, *Dynamical Evidence For a Fifth Force Explanation of the ATOMKI Nuclear Anomalies*, *Phys. Rev. D* **102** (2020) 036016, [2006.01151].
- [26] NA48/2 collaboration, J. Batley et al., *Search for the dark photon in π^0 decays*, *Phys. Lett. B* **746** (2015) 178–185, [1504.00607].
- [27] R. Essig et al., *Working Group Report: New Light Weakly Coupled Particles*, in *Community Summer Study 2013: Snowmass on the Mississippi*, 10, 2013, 1311.0029.
- [28] H. Davoudiasl, H.-S. Lee and W. J. Marciano, *Muon $g - 2$, rare kaon decays, and parity violation from dark bosons*, *Phys. Rev. D* **89** (2014) 095006, [1402.3620].
- [29] A. N. Khan, *Global analysis of the source and detector nonstandard interactions using the short baseline ν - e and $\bar{\nu}$ - e scattering data*, *Phys. Rev. D* **93** (2016) 093019, [1605.09284].
- [30] L.-M. Gu, H.-B. Li, X.-X. Ma and M.-Z. Yang, *Study of the electromagnetic Dalitz decays $\psi(\Upsilon) \rightarrow \eta_c(\eta_b) l^+ l^-$* , *Phys. Rev. D* **100** (2019) 016018, [1904.06085].
- [31] J. Fu, H.-B. Li, X. Qin and M.-Z. Yang, *Study of the Electromagnetic Transitions $J/\psi \rightarrow Pl^+ l^-$ and Probe Dark Photon*, *Mod. Phys. Lett. A* **27** (2012) 1250223, [1111.4055].
- [32] CLEO collaboration, R. Mitchell et al., *J/ψ and $\psi(2S)$ Radiative Decays to $\eta(c)$* , *Phys. Rev. Lett.* **102** (2009) 011801, [0805.0252].

- [33] V. Anashin et al., *Measurement of $J/\psi \rightarrow \eta_c \gamma$ at KEDR*, *Chin. Phys. C* **34** (2010) 831–835, [1002.2071].
- [34] D. Becirevic and F. Sanfilippo, *Lattice QCD study of the radiative decays $J/\psi \rightarrow \eta_c \gamma$ and $h_c \rightarrow \eta_c \gamma$* , *JHEP* **01** (2013) 028, [1206.1445].
- [35] E. Kou, P. Urquijo, W. Altmannshofer, F. Beaujean, G. Bell, M. Beneke et al., *The Belle II Physics Book, Progress of Theoretical and Experimental Physics* **2019** (Dec, 2019) .
- [36] BESIII collaboration, M. Ablikim et al., *Measurements of the branching fractions of $\eta_c \rightarrow K^+ K^- \pi^0$, $K_S^0 K^\pm \pi^\mp$, $2(\pi^+ \pi^- \pi^0)$, and $p\bar{p}$* , *Phys. Rev. D* **100** (2019) 012003, [1903.05375].
- [37] R. Barbieri and T. E. O. Ericson, *Evidence Against the Existence of a Low Mass Scalar Boson from Neutron-Nucleus Scattering*, *Phys. Lett. B* **57** (1975) 270–272.
- [38] J. Alwall, R. Frederix, S. Frixione, V. Hirschi, F. Maltoni, O. Mattelaer et al., *The automated computation of tree-level and next-to-leading order differential cross sections, and their matching to parton shower simulations*, *JHEP* **07** (2014) 079, [1405.0301].
- [39] A. Alloul, N. D. Christensen, C. Degrande, C. Duhr and B. Fuks, *FeynRules 2.0 - A complete toolbox for tree-level phenomenology*, *Comput. Phys. Commun.* **185** (2014) 2250–2300, [1310.1921].
- [40] BELLE II collaboration, I. Adachi et al., *Search for an Invisibly Decaying Z' Boson at Belle II in $e^+e^- \rightarrow \mu^+\mu^-(e^\pm\mu^\mp)$ Plus Missing Energy Final States*, *Phys. Rev. Lett.* **124** (2020) 141801, [1912.11276].
- [41] BELLE-II collaboration, W. Altmannshofer et al., *The Belle II Physics Book*, *PTEP* **2019** (2019) 123C01, [1808.10567].
- [42] K. Hanagaki, H. Kakuno, H. Ikeda, T. Iijima and T. Tsukamoto, *Electron identification in Belle*, *Nuclear Instruments and Methods in Physics Research Section A: Accelerators, Spectrometers, Detectors and Associated Equipment* **485** (2002) 490–503.
- [43] V. Bertacchi, T. Bilka, N. Braun, G. Casarosa, L. Corona, S. Cunliffe et al., *Track finding at Belle II*, *Computer Physics Communications* **259** (Feb, 2021) 107610.
- [44] M. Duerr, T. Ferber, C. Hearty, F. Kahlhoefer, K. Schmidt-Hoberg and P. Tunney, *Invisible and displaced dark matter signatures at Belle II*, *JHEP* **02** (2020) 039, [1911.03176].